J. Fluid Mech. (1991), *vol.* 232, *pp.* 73–98
Printed in Great Britain

Eddy-viscosity and drag-law models for random ocean wave dissipation

By S. L. WEBER
Royal Netherlands Meteorological Institute, P.O. Box 201, 3730 AE De Bilt, The Netherlands

(Received 23 January 1989 and in revised form 3 December 1990)

The spectral energy dissipation of finite-depth ocean waves, due to friction in the turbulent bottom boundary layer, is investigated using a formal parameterization of the turbulent stress. This formal parameterization is a generalization from both the eddy-viscosity model and the drag law. The eddy-viscosity model is linear in the random wave phase, whereas the drag law is nonlinear. The phase dependency of the stress is found to determine the form of the dissipation expression. A spectral eddy-viscosity model developed by the author, an eddy-viscosity model based on an 'equivalent' monochromatic wave given by Madsen *et al.* (1989), the drag law as applied by Hasselmann & Collins (1968) and an approximation to the Hasselmann & Collins expression given by Collins (1972) are discussed within the framework of the formal parameterization. Some examples of applications are given.

1. Introduction

Surface gravity waves, with a wavelength which is long compared to the water depth, give rise to a thin wave boundary layer at the sea bottom. This boundary layer is characterized by a steep vertical gradient of the horizontal velocity, and is generally turbulent under field conditions. When the bottom material consists of sand, the wave and sand motion will interact and ripples may form. These increase the bottom roughness experienced by the waves. The waves lose energy due to turbulent friction in the bottom boundary layer.

One of the earliest studies on the monochromatic wave boundary layer is Kajiura (1968), who showed that the energy dissipation is to first order in wave steepness a function of the bottom stress only. Kajiura used a linear eddy-viscosity model, with a prescribed vertical profile for the eddy-viscosity coefficient, to describe the turbulent stress. The eddy-viscosity model was extended by Grant & Madsen (1979) and by Christoffersen & Jonsson (1985) to a combined (monochromatic) wave–current flow. Grant & Madsen (1982) developed an eddy-viscosity model for the sediment–wave interaction. Nonlinear eddy-viscosity models, with time-varying coefficients, were developed by Lavelle & Mofjeld (1983) and Trowbridge & Madsen (1984). The latter showed that the wave energy dissipation is adequately described using only the time-independent part of the eddy-viscosity coefficient. In all eddy-viscosity models analytical solutions are combined with iterative schemes.

An example of a purely numerical model is that put forward by Davies, Soulsby & King (1988), who determine the eddy-viscosity coefficient from the turbulent kinetic energy equation. The numerical model developed by Bakker & van Doorn (1979) uses the mixing-length hypothesis. The simplest turbulence model is the drag law, with an experimentally determined drag coefficient (see for example Jonsson

1980). Jonsson gives an extensive overview of previous experimental and theoretical studies on monochromatic-wave boundary layers; references to more recent work can be found in Davies *et al.* (1988).

The basic concepts of all turbulence models mentioned were originally developed for stationary, constant-stress boundary layers. Recent experiments (Hino *et al.* 1983; Sleath 1987) with direct measurements of the turbulence characteristics in monochromatic-wave boundary layers show significant differences as compared to steady flows. Negative and time-varying eddy-viscosity coefficients had been found before (Horikawa & Watanabe 1968; Jonsson 1980). Unfortunately, a definite parameterization of the oscillatory turbulent bottom stress does not exist and modelling of the wave boundary layer is generally based on the closure schemes mentioned or on extensions thereof.

The frictional energy loss of random ocean waves is an important dissipation mechanism in shallow-water areas. There has been surprisingly little research on the random-wave boundary layer, either theoretically or experimentally. The first paper on bottom friction which deals explicitly with the stochastic nature of the wave field is Hasselmann & Collins (1968). They substitute a quadratic drag law in the general expression for the wave energy dissipation in terms of the bottom stress. Their theory predicts a pronounced influence of the mean current on the wave energy dissipation, which was not confirmed by measurements (JONSWAP 1973). Hasselmann & Collins proposed the use of a constant drag coefficient. An estimate of the value of the drag coefficient for different data sets is given by Shemdin *et al.* (1978); the values range from 0.006 to 0.1. Notwithstanding these drawbacks the Hasselmann & Collins expression is used in various wave forecasting models, mostly in a simplified version given by Collins (1972).

More sophisticated turbulence models have been developed for the oscillatory boundary layer since the appearance of Hasselman & Collins' paper. An obvious alternative for the drag law is the linear eddy-viscosity model. This parameterization allows an analytical solution of the boundary-layer equations. It is therefore easy to apply the subsequent expression for the energy dissipation in a wave forecasting model.

The dissipation expression, which can be computed from the eddy-viscosity model, differs significantly from the Hasselmann & Collins expression. This is somewhat surprising, as the eddy-viscosity concept is compatible with a drag law for stationary flows. For monochromatic waves there is a phase shift in the eddy-viscosity model between the bottom stress and the free-stream velocity, which does not appear in the drag law (see for example Visser 1988). In the case of a random wave field the discrepancy between these two concepts is even larger.

In the present paper the energy dissipation due to bottom friction is studied using a formal parameterization of the turbulent stress, which is a generalization both from the eddy-viscosity model and from the drag law. The differences between the two models can be explained from the generalized parameterization. They are partly due to the different ways in which the stress is related to the non-dimensional bottom roughness length. More important, is whether the stress depends linearly or nonlinearly on the random wave phase.

Two eddy-viscosity models and the drag law are discussed as special cases of this generalized parameterization. One eddy-viscosity model was developed by the author, the other by Madsen, Poon & Graber (1989). The model by Madsen *et al.* differs in a number of respects from the present model. Moreover, their approach is directed at representing the random wave field by an 'equivalent' monochromatic

wave, whereas the present model retains a spectral description. The present model is therefore more widely applicable; it can be used in complicated situations like a turning wind field or swell interacting with wind–sea, where the wave field cannot be represented by a monochromatic wave.

The generalized parameterization does not take the purely numerical models into account. To investigate these models, one would have to consider them separately for selected cases. This was done for a number of combined monochromatic wave–current situations by Dyer & Soulsby (1988).

In the present paper a theoretical framework is constructed for the dissipation of random ocean waves due to turbulent bottom friction. The dissipation is determined by explicitly computing the modifications in the fluid flow due to the presence of the boundary. This is done in terms of the (basically unknown) bottom stress and the (known) zero-order flow outside the boundary layer. Assuming that the stress can be parameterized in terms of the zero-order flow, the dissipation can be computed. Various approaches to the modelling of the turbulent stress (linear versus nonlinear, spectral versus 'equivalent' monochromatic) will be discussed.

Some examples of the application of the bottom friction models are also given. These show that a dissipation function based on the eddy-viscosity concept is a good alternative to the Hasselmann & Collins expression, which has been widely applied in wave modelling. A more extensive evaluation is given by Weber (1991).

The plan of this paper is as follows. In §2 the boundary-layer equations are derived, using linear wave theory. The basic expression for the energy dissipation in terms of the bottom stress is determined. In §3 the generalized parameterization is defined and the structure of the dissipation function is analysed. Examples of the generalized parameterization are discussed in §4. Finally all results are summarized in §5. All the calculus related to the averaging of random quantities is given in the Appendix.

2. Wave energy dissipation as a function of the bottom stress

2.1. *The turbulent bottom boundary layer*

Consider an inviscid, incompressible fluid, with the velocity field given by the equations for conservation of mass and momentum, the condition of zero normal velocity at the bottom and at the free surface and continuity of pressure across the free surface. In finite-depth water this velocity field has non-zero horizontal velocity components at the bottom, while in reality the viscosity of the water, however small it may be, imposes the no-slip condition. To fulfil this condition the concept of a boundary layer is needed: an essentially small region close to the bottom, where the horizontal velocity increases rapidly from zero at the bottom to a finite value, determined by the outer flow, at the top.

A boundary-layer Reynolds number can be defined by

$$R = \frac{Ud}{\nu}.$$

Here U is a characteristic scale for the horizontal velocity, d a characteristic length in the transverse direction and ν the kinematic viscosity of the fluid ($\nu \approx 10^{-6}$ m^2/s). I will consider flows with $U > 0.1$ m/s and $d > 0.1$ m, so that $R > 10^4$. This implies that the boundary layer is fully turbulent for flows over a rough bed (Jonsson 1980). In the following only turbulent flows over rough surfaces will be considered.

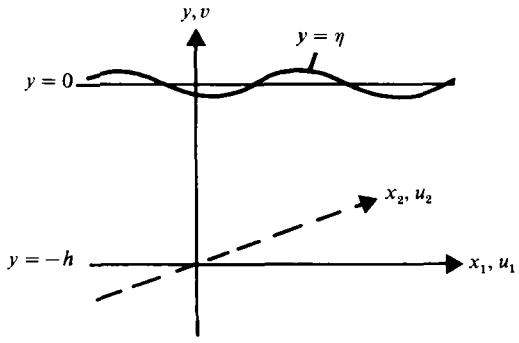

FIGURE 1. Definition of the coordinate system.

A lengthscale k_N can be associated with the roughness elements on the sea bed (sand grains, gravel, ripples). In the case of flow over a rough surface k_N is much larger than the lengthscale ν/u^* that characterizes the thickness of the viscous sublayer. Here u^* is a velocity that represents the turbulence intensity. Therefore k_N is the only lengthscale for the flow close to the bottom. The no-slip condition is applied at a theoretical zero level $k_N/30$, where k_N has to be determined experimentally as a function of the roughness elements (Schlichting 1955). In the case of rough turbulent flow the viscous stresses can be neglected everywhere.

The turbulent stress tensor is an additional unknown in the equations for the fluid motion. Additional assumptions are needed now to solve the equations. In this section the turbulent stress will be left as an unknown in the equations of motion. It will be shown that the equations suggest a certain form of stress parameterization; this will be pursued further in §3. Examples will be treated in §4. In this section the wave energy dissipation due to friction in the turbulent boundary layer will be derived to first order in wave steepness as a function of the turbulent bottom stress.

In the following the (Reynolds averaged) velocity will be denoted by $\boldsymbol{u} = (u_1, u_2, v)$, the space coordinate by $\boldsymbol{x} = (x_1, x_2, y)$ and the free surface by $y = \eta$ (see figure 1); h is the water depth. The stress tensor is given by:

$$\frac{\tau_{ij}}{\rho} = -\overline{u_i' u_j'},$$

where ρ is the density of water and u_i' $(i = 1, 3)$ is the turbulent fluctuation in the velocity in the ith direction. The overbar stands for Reynolds averaging. For notational convenience ρ will be absorbed in the stress in the remainder of this paper.

Correct to first order in wave steepness the fluid flow is given by

$$\left.\begin{aligned} \nabla \cdot \boldsymbol{u} &= 0, \\ \frac{\partial u_i}{\partial t} &= -\frac{1}{\rho}\frac{\partial p}{\partial x_i} + \frac{\partial \tau_{ij}}{\partial x_j}, \end{aligned}\right\} \tag{2.1a}$$

with boundary conditions

$$\text{at } y = 0: \qquad \eta_t = v; \quad p - g\rho\eta = 0 \tag{2.1b}$$

$$\text{at the bottom:} \qquad u_1 = u_2 = v = 0 \tag{2.1c}$$

p is the pressure, t is time and g is the gravitational acceleration. In (2.1a) summation over repeated indices is implied.

2.2. *An asymptotic expansion of the velocity*

The boundary layer is characterized by steep gradients in the vertical direction, but slow change in the horizontal direction. The ratio between the vertical lengthscale, say the boundary-layer thickness, and the horizontal lengthscale, say a wavelength, defines a small dimensionless parameter which will be denoted by δ. The steepness of the vertical gradients can be expressed explicitly by introducing a stretched coordinate $z = (y+h)/\delta$. Variables which change rapidly through the boundary layer are made to depend on z. It follows that

$$\frac{\partial}{\partial y} = \frac{1}{\delta}\frac{\partial}{\partial z}.$$

The velocity field can be written as the sum of an irrotational part, which depends on the original coordinate y, and a solenoidal part, which depends on the magnified coordinate z:

$$\boldsymbol{u} = \nabla\phi + \nabla \times \boldsymbol{\psi},$$

where ϕ is the velocity potential and $\boldsymbol{\psi} = (\psi_1, \psi_2, \psi_3)$ is the vector stream function. The rotation in the velocity field is induced by the turbulent stress τ_{ij}. Let the pressure be determined by the irrotational part: $p = -\rho\phi_t$. The bottom boundary condition is applied at $y = -h$ and $z = z_0 = k_N/(30\delta)$.

The surface elevation and the velocity components are expanded in terms of δ to determine an approximate solution of (2.1*a*) that is valid everywhere and that satisfies all boundary conditions. This composite asymptotic expansion is combined with a multiple-timescale method. (See Nayfeh 1973 for an overview of expansion techniques.) Thus the order-δ^{n-1} solution is valid for times up to order $1/\delta^n$. The expansion reads

$$\left.\begin{aligned} \eta &= \eta^0 + \delta\eta^1 + \ldots, \\ \phi &= \phi^0 + \delta\phi^1 + \ldots, \\ \boldsymbol{\psi} &= \delta\boldsymbol{\psi}^1 + \ldots. \end{aligned}\right\} \tag{2.2}$$

η, ϕ and $\boldsymbol{\psi}$ depend explicitly on a slow time variable $s = \delta t$, as well as on the (ordinary) time t.

The composite solution must reduce to the inviscid wave solution if the boundary-layer thickness tends to zero:

$$\lim_{\delta \downarrow 0} \boldsymbol{u} = \nabla\phi^0 \quad \text{(for fixed } y\text{)} \tag{2.3}$$

It follows from (2.3) that the stream function can be chosen such that $\boldsymbol{\psi}^0 = 0$. The solution for the boundary-layer flow can be found by taking the limit $\delta \downarrow 0$ for fixed z.

One can assume that the vertical variations in the turbulent stresses are much larger than the horizontal variations, so that the stress gradients $\partial\tau_{i3}/\partial z$ are the dynamically important quantities in (2.1*a*). These are of zero order. Therefore the stress tensor elements are of order δ at most (assuming all stresses to have the same order of magnitude). The shear stresses τ_{i3}, which appear in the equations for the horizontal velocity, will be denoted by $\tau_i (i = 1, 2)$, with

$$\tau_i = \delta\tau_i^1 + \ldots. \tag{2.4}$$

The zero-order and the order-δ equations are found by substitution of the expansions (2.2) and (2.4) in the flow equations (2.1) and (2.3). The order-δ equations are only given in so far as they are needed to determine the dependence of the surface elevation and the velocity on the slow-time variable s.

Zero-order equations:

$$\nabla^2\phi^0 = 0 \tag{2.5a}$$

at $y = 0$: $$\phi^0_{tt} + g\phi^0_y = 0, \quad \eta^0_t = \phi^0_y; \tag{2.5b}$$

at $y = -h, z = z_0$: $$\phi^0_y = 0, \quad \phi^0_{x_1} - \psi^1_{2z} = 0, \quad \phi^0_{x_2} + \psi^1_{1z} = 0; \tag{2.5c}$$

for fixed y: $$\lim_{\delta \downarrow 0} \psi^1_{1z} = \lim_{\delta \downarrow 0} \psi^1_{2z} = 0. \tag{2.5d}$$

Order-δ equations:

$$\nabla^2\phi^1 = 0, \qquad \psi^1_{2t} = -\tau^1_1, \quad \psi^1_{1t} = \tau^1_2; \tag{2.6a}$$

at $y = 0, z \to \infty$: $$2g\eta^0_s = \phi^1_{tt} + g\phi^1_y \tag{2.6b}$$

at $y = -h, z = z_0$: $$\phi^1_y + \psi^1_{2x_1} - \psi^1_{1x_2} = 0 \tag{2.6c}$$

2.3. *Zero-order solution*

At zero order the inviscid, non-turbulent equations are recovered for η^0 and ϕ^0. I am looking for wave solutions of the form

$$\eta^0 = \sum_k \eta^0_k = \sum_k \tilde{\eta}^0_k + \text{c.c.}, \quad \phi^0 = \sum_k \phi^0_k = \sum_k \tilde{\phi}^0_k + \text{c.c.}, \tag{2.7}$$

where c.c. denotes complex conjugate. From (2.5*a–c*) $\tilde{\eta}^0_k$ and $\tilde{\phi}^0_k$ are found as

$$\tilde{\eta}^0_k = \tfrac{1}{2}A_k e^{i\theta_k}, \quad \tilde{\phi}^0_k = -i\frac{\omega}{k}\frac{\cosh k(y+h)}{\sinh kh}\tilde{\eta}^0_k. \tag{2.8}$$

$\theta_k = k_1 x_1 + k_2 x_2 - \omega t$, with $\boldsymbol{k} = (k_1, k_2)$ the wavenumber vector with modulus $k = (k_1^2 + k_2^2)^{\frac{1}{2}}$ and ω the radian frequency, given by $\omega^2 = gk \tanh kh$. The wave steepness is defined as $A_k k$.

The no-slip condition is not fulfilled by the inviscid solution given by ϕ^0. Therefore there is a zero-order correction to the inviscid tangential velocity denoted by $\psi^1_{iz} (i = 1, 2)$. Away from the bottom the correction velocity vanishes according to the boundary condition (2.5*d*). At zero order the presence of the boundary modifies only the horizontal flow close to the boundary. The boundary-layer correction to the horizontal velocity gives rise to a vertical velocity component, because of continuity of mass. This 'correction' in the vertical velocity has to be of order δ, since the vertical lengthscale is of order δ compared to the horizontal lengthscale. The no-slip boundary condition, which is imposed on the zero-order horizontal velocity, thus results in the boundary condition (2.6*c*) on the order-δ vertical velocity.

2.4. *Order-δ solution*

The stresss $\boldsymbol{\tau}^1$, which forces the rotational correction velocity in the boundary layer, is essentially unknown. Presumably $\boldsymbol{\tau}^1$ is connected with the large gradient in the horizontal velocity in the boundary layer. It is assumed that $\boldsymbol{\tau}^1$ can be parameterized in terms of the outer flow, which was written as a sum of harmonics of the form $\exp(i\theta_k)$ in the previous section. The parameterization need not be linear. The stress is in a very complicated way nonlinear in, for example, the case of a drag law (see

§4.3); τ^1 can therefore contain terms other than these 'first harmonics'. The terms in τ^1 can be of the order δ at most, but it is not possible to say *a priori* if there is any ordering among them.

The boundary condition (2.5*c*) imposes terms of the form $\exp(\mathrm{i}\theta_k)$ in ψ_i^1, so that ϕ^1 and τ_i^1 have to contain these too. The time dependence of possible other terms in ϕ^1 is determined by the boundary condition (2.6*b*). Secular terms in the solution are avoided by equating the first harmonics on the right-hand side of (2.6*b*) to $2g\eta_s^0$. The aim of this section is to determine the slow wave-amplitude attenuation η_s^0. It is clear now that only the first harmonics have to be taken into account in order to do this. Only terms of the form $\exp(\mathrm{i}\theta_k)$ will therefore be considered in this section.

The horizontal derivatives of ϕ^0, which occur in the bottom boundary condition (2.5*c*), denote the zero-order free-stream velocity at the top of the bottom boundary layer $\boldsymbol{U} = (U_1, U_2, 0)$, with

$$U_{ik} = \frac{\partial}{\partial x_i}\phi_k^0 = \frac{k_i}{k}\frac{\omega}{\sinh kh}\tilde{\eta}_k^0 + \text{c.c.} = \frac{k_i}{k}\tilde{U}_k + \text{c.c.} \tag{2.9}$$

Because of this boundary condition, the first harmonics of the stream function will be expressed in terms of $\tilde{U}_k$ as

$$\psi_{1k}^1 = \frac{\mathrm{i}}{k}T_k(z)\frac{k_2}{k}\tilde{U}_k + \text{c.c.}, \quad \psi_{2k}^1 = -\frac{\mathrm{i}}{k}T_k(z)\frac{k_1}{k}\tilde{U}_k + \text{c.c.} \tag{2.10}$$

The z-dependence of the (first harmonics of the) stress and the stream function cannot be solved from the present equations, as there is only one equation, (2.6*a*), for two unknowns. The T_k express our ignorance of the stress and the velocity profile in the boundary layer. The boundary conditions (2.5*c*) and (2.5*d*) now reduce to conditions on the unknown function T_k:

$$T_{kz}(z_0) = \mathrm{i}k, \qquad \lim_{\delta \downarrow 0} T_{kz} = 0. \tag{2.11}$$

From the boundary-layer equations (2.6*a*) and from (2.10) the first harmonics of the stress can be expressed as

$$\tau_{ik}^1 = \frac{\omega}{k}T_k(z)\frac{k_i}{k}\tilde{U}_k + \text{c.c.} \tag{2.12}$$

The first-harmonics part of ϕ^1 is found from the Laplace equation (2.6*a*), the bottom boundary condition (2.6*c*) and (2.10) as

$$\phi_k^1 = \frac{1}{k}T_k(z_0)\,\mathrm{e}^{-k(y+h)}\tilde{U}_k + \text{c.c.} \tag{2.13}$$

Finally the slow wave-amplitude attenuation follows from (2.6*b*) and (2.13) as

$$\frac{\partial}{\partial s}\tilde{\eta}_k^0 = -\frac{1}{2}\frac{1}{\cosh kh}T_k(z_0)\tilde{U}_k. \tag{2.14}$$

This expression will be used in the next subsection to derive the frictional attenuation of the surface elevation spectrum.

It is of interest to compute the order-δ velocity and pressure outside the boundary layer. The order-δ vertical velocity is non-zero at the top of the boundary layer. In the interior of the flow the horizontal and the vertical scales are equal, so that an

order-δ vertical velocity gives rise to an order-δ horizontal velocity (through continuity of mass). The small change in the velocity field accompanies a small modification in the pressure. The modifications can be expressed in terms of the bottom stress, using (2.12) and (2.13), as

$$u_{ik}^1 = \frac{\partial}{\partial x_i}\phi_k^1 = \mathrm{i}\frac{k_i}{k}\frac{\mathrm{e}^{-k(y+h)}}{\omega/k}\tilde{\tau}_k^1(z_0) + \text{c.c.},$$

$$v_k^1 = \frac{\partial}{\partial y}\phi_k^1 = -\frac{\mathrm{e}^{-k(y+h)}}{\omega/k}\tilde{\tau}_k^1(z_0) + \text{c.c.},$$

$$\frac{1}{\rho}p_k^1 = -\frac{\partial}{\partial t}\phi_k^1 = \mathrm{i}\,\mathrm{e}^{-k(y+h)}\tilde{\tau}_k^1(z_0) + \text{c.c.}$$

The induced order-δ bottom velocity is one order of magnitude smaller than the bottom stress, as the wave phase velocity ω/k is typically 10 m/s. The order-δ bottom pressure equals the bottom stress, except for a phase lag. One can physically picture how these modifications, which are due to the presence of the boundary, slowly work their way up through the water column and finally modify the surface elevation.

2.5. *The spectral energy dissipation*

The random nature of the surface displacement is expressed by a random phase angle in (2.8):

$$A_k = \hat{A}_k \mathrm{e}^{\mathrm{i}\epsilon_k},$$

where the amplitudes $\hat{A}_k$ are chosen such that $\hat{A}_k^2 = 2F(\boldsymbol{k})\,\Delta\boldsymbol{k}$, with $F(\boldsymbol{k})$ the energy density at the wavenumber $\boldsymbol{k}$ and $\Delta\boldsymbol{k}$ the wavenumber increment. The ϵ_k are independent and distributed uniformly over the interval $(0, 2\pi)$. The mean wave amplitudes are therefore zero. The second moment is only non-zero if a wave component is paired with its complex conjugate:

$$\langle \tilde{\eta}_k^0 \tilde{\eta}_k^{0*} \rangle = \tfrac{1}{2}F(\boldsymbol{k})\,\Delta\boldsymbol{k}, \tag{2.15}$$

where $\langle \cdot \rangle$ stands for ensemble averaging and * denotes the complex conjugate.

Rice (1944, 1945) has shown that the distribution function of the surface elevation η approaches a normal law, as the number of wave components tends to infinity and $\Delta\boldsymbol{k}$ tends to zero.

The linear series (2.7) is a first-order (in wave steepness) approximation to the random surface elevation. In order to satisfy the nonlinear boundary conditions at the sea surface one has to add terms which are quadratic in the wave amplitudes and higher-order terms. The dynamical effects of these nonlinear terms will be discussed briefly in §4.4.1. The distribution function of the nonlinear series for η is given by a Gram–Charlier series (Longuet-Higgins 1963). At first order this series reduces to the Gaussian distribution. There seems to be a second source of nonlinearities if the turbulent boundary layer at the bottom is taken into account: the stress term in the boundary-layer equations. The turbulent stress has however no direct effect on the zero-order flow outside the boundary layer. The free-stream velocity is therefore jointly Gaussian at first order in wave steepness and zero order in δ.

At present it is assumed that there is a parameterization of the stress in terms of the free-stream bottom velocity, as stated earlier. Under this assumption the stress inherits its stochastic characteristics from U. This does not imply that the stress components are independent, as a given stress components can contain information

from different velocity components. It would be convenient to have an expression for the turbulent stress that fits in with an expansion in the wave steepness, as commonly applied in wave dynamics. This can be achieved by expanding the stress in a Taylor series around the velocity field with one specific component U_k set to zero (Beran 1968):

$$\tau_i^1 = \tau_i^1(U_k = 0) + \tilde{U}_k \frac{\partial}{\partial \tilde{U}_k} \tau_i^1(U_k = 0) + \tilde{U}_k^* \frac{\partial}{\partial \tilde{U}_k^*} \tau_i^1(U_k = 0) + \ldots. \tag{2.16}$$

Multiplying this expression with $\tilde{U}_k^*$ and averaging it follows that the coefficients of the first harmonics in τ are given by

$$\frac{\langle \tau_i^1 \tilde{U}_k^* \rangle}{\langle \tilde{U}_k \tilde{U}_k^* \rangle} = \left\langle \frac{\partial}{\partial \tilde{U}_k} \tau_i^1(U_k = 0) \right\rangle. \tag{2.17}$$

Terms of order $(\Delta k)^2$ and higher, which follow from the fourth- and higher-order even moments, are neglected here. The Taylor expansion can be repeated for a second component U_l. Multiplying this second expansion with $\tilde{U}_l^*$ and again averaging one finds the coefficients of the terms $U_k U_l$. These are of second order in wave steepness and can be neglected here.

Comparing (2.17) with the notation (2.12) for the first harmonics of the stress one finds that

$$\frac{\omega}{k} T_k \frac{k_i}{k} = \left\langle \frac{\partial}{\partial \tilde{U}_k} \tau_i^1(U_k = 0) \right\rangle.$$

It follows that

$$\frac{\omega}{k} T_k = \frac{\boldsymbol{k}}{k} \cdot \left\langle \frac{\partial}{\partial \tilde{U}_k} \boldsymbol{\tau}^1 \right\rangle. \tag{2.18}$$

Here the dot denotes the inner product.

Substituting (2.18) back in (2.12) the turbulent stress can be written in an implicit form as

$$\tau_i^1 = \sum_k \left\{ \frac{\boldsymbol{k}}{k} \cdot \left\langle \frac{\partial}{\partial \tilde{U}_k} \boldsymbol{\tau}^1 \right\rangle \right\} \frac{k_i}{k} \tilde{U}_k + \text{c.c.} \tag{2.19}$$

This formula will be used in §3 to determine the first-harmonics part of the stress in the case of a nonlinear parameterization.

The spectral energy dissipation can now be computed from (2.14), using (2.9), (2.15) and (2.18), as

$$\frac{\partial}{\partial s} F(\boldsymbol{k}) \Delta \boldsymbol{k} = -\left\{ \frac{\boldsymbol{k}}{k} \cdot \left\langle \frac{\partial}{\partial \tilde{U}_k} \boldsymbol{\tau}^1(z_o) \right\rangle + \text{c.c.} \right\} \frac{k}{\sinh 2kh} F(\boldsymbol{k}) \Delta \boldsymbol{k}. \tag{2.20}$$

The dissipation rate is thus found to be proportional to the bottom velocity spectrum, with the proportionality factor given by the functional derivative of the bottom stress. The same factor occurs in the implicit parameterization (2.19), which relates the stress to the free-stream velocity. The dependence of the dissipation rate on the form of the stress parameterization will be investigated in the next section, using (2.19) and (2.20).

The dissipation (2.20) can be rewritten, using (2.9), (2.15) and (2.17), as

$$\frac{\partial}{\partial s} F(\boldsymbol{k}) \Delta \boldsymbol{k} = -\frac{1}{g} \langle \boldsymbol{\tau}^1(z_0) \cdot \boldsymbol{U}_k \rangle. \tag{2.21}$$

This yields the dissipation by bottom friction as the work done by the bottom stress against the velocity component U_k. This could have been derived directly from the momentum equation (2.1a), as was done by Kajiura (1968) and Hasselmann & Collins (1968). The foregoing analysis has revealed the mechanism by which the dissipation takes place: the retardation of the horizontal velocity in the bottom boundary layer goes with an order-δ modification in the velocity and the pressure in the outer flow. These extend up to the surface and slowly modify the surface elevation. Only the first harmonics of the bottom stress actually work on the mean flow. This was to be expected, as only the first harmonics of the velocity and the pressure in the outer flow were considered.

The dissipation expression derived here is valid to first order in wave steepness, under very general conditions for the turbulent boundary layer. One assumes that the stress can be parameterized in terms of the outer flow, that the flow is fully rough turbulent and that the boundary-layer thickness is small compared to a wavelength.

3. Generalized parameterization of the turbulent stress

3.1. *Definition of the generalized parameterization*

In this section a formal parameterization of the turbulent shear stress $\tau = (\tau_1, \tau_2)$ is defined. The expression (2.12), which was derived in the previous section, suggests a certain form of stress parameterization. This form is used here. I will use a 'linear' and a 'nonlinear' formulation for the stress; the adjectives refer to the stochastic characteristics of the stress parameterization. A linear parameterization is linear in the random wave phase, so that the stress is jointly Gaussian. A nonlinear parameterization is nonlinear in the random wave phase; it can be linearized using (2.19). A generalized expression is used here in order to investigate the dependence of the energy dissipation on the stochastic characteristics of the stress.

Consider the following class of parameterizations:

$$\tau_i(z) = \langle \tau_0^{\frac{1}{2}} \rangle \sum_k \frac{k_i}{k} T_k(z)\, \tilde{U}_k + \text{c.c.} \quad \text{(linear)}, \tag{3.1a}$$

$$\tau_i(z) = \tau_0^{\frac{1}{2}} \sum_k \frac{k_i}{k} T_k(z)\, \tilde{U}_k + \text{c.c.} \qquad \text{(nonlinear)}, \tag{3.1b}$$

with $\tau_0 = [\tau_1^2(z_0) + \tau_2^2(z_0)]^{\frac{1}{2}}$. The velocity scale ω/k, which occurs in (2.12), is replaced by the average friction velocity $\langle \tau_0^{\frac{1}{2}} \rangle$ in the linear formulation (3.1a). An obvious generalization to a nonlinear parameterization is by using the instantaneous friction velocity $\tau_0^{\frac{1}{2}}$. In the nonlinear case (3.1b) the first-harmonics part of the stress can be determined from (2.19). With this definition of the velocity scale the parameterizations (3.1a, b) are generalizations from the eddy-viscosity model and the drag law. The unknown function T_k will be specified in §4, where these examples are discussed. In the remainder of this section only the bottom stress is considered, so that T_k always denotes $T_k(z_0)$ and τ denotes $\tau(z_0)$.

A variable $t = (t_1, t_2)$, which is linear in the random wave phase, can be defined from (3.1a, b) as follows:

$$t_i(z_0) = \sum_k T_k(z_0) \frac{k_i}{k} \tilde{U}_k + \text{c.c.} \tag{3.2}$$

This implies that

$$t_i = \frac{\tau_i}{\langle \tau_0^{\frac{1}{2}} \rangle} \quad \text{(linear)}, \tag{3.3a}$$

$$t_i = \frac{\tau_i}{\tau_0^{\frac{1}{2}}} \quad \text{(nonlinear)}. \tag{3.3b}$$

t_1 and t_2 are jointly Gaussian, as the velocity components $\tilde{U}_k$ are statistically independent. Their joint distribution function is

$$f(t_1, t_2) = \frac{1}{2\pi(\sigma_{11}\sigma_{22})^{\frac{1}{2}}} \exp\left[-\frac{1}{2}\left(\frac{t_1^2}{\sigma_{11}} + \frac{t_2^2}{\sigma_{22}}\right)\right], \tag{3.4}$$

with

$$\sigma_{ij} = \langle t_i t_j \rangle = \int_k \frac{k_i k_j}{k^2} T_k T_k^* \frac{\omega^2}{\sinh^2 kh} F(\boldsymbol{k})\, \mathrm{d}\boldsymbol{k}. \tag{3.5}$$

Without loss of generality the horizontal coordinate system at the bottom can be chosen such that $\sigma_{12} = 0$ and $\sigma_{22} \leqq \sigma_{11}$ (see the Appendix).

The average derivatives of the bottom stress can now be computed from (3.1*a*, *b*). Expressing these quantities in terms of t instead of τ, they can be evaluated explicitly in terms of the variances σ_{11} and σ_{22} by means of the known Gaussian distribution function of t. All the details of the following calculations are given in the Appendix.

3.2. *The average derivatives of the bottom stress*

The computation of the average derivatives is straightforward in the linear case. It follows from (3.1*a*) and (3.3*a*) that

$$\left\langle \frac{\partial}{\partial \tilde{U}_k} \tau_i \right\rangle = \langle \tau_0^{\frac{1}{2}} \rangle \frac{k_i}{k} T_k = \langle t^{\frac{1}{2}} \rangle^2 \frac{k_i}{k} T_k, \tag{3.6}$$

with

$$\langle t^{\frac{1}{2}} \rangle^2 = \sigma_{11}^{\frac{1}{2}} \Gamma(\tfrac{5}{4})^2 \sqrt{2} F(-\tfrac{1}{4}, \tfrac{1}{2}, 1, A)^2 =: \sigma_{11}^{\frac{1}{2}} F_3(A). \tag{3.7}$$

Here F is a hypergeometric function (Abramowitz & Stegun 1965) with argument $A = 1 - \sigma_{22}/\sigma_{11}$; A characterizes the directional spread of the bottom stress spectrum. (The left-hand side of (3.7) defines F_3 on the right-hand side.)

One then finds that

$$\frac{\boldsymbol{k}}{k} \cdot \left\langle \frac{\partial}{\partial \tilde{U}_k} \boldsymbol{\tau} \right\rangle = \langle \tau_0^{\frac{1}{2}} \rangle T_k = \sigma_{11}^{\frac{1}{2}} F_3(A)\, T_k. \tag{3.8}$$

In the nonlinear case the computation is complicated by the factor $\tau_0^{\frac{1}{2}}$ in (3.1*b*):

$$\left\langle \frac{\partial}{\partial \tilde{U}_k} \tau_j \right\rangle = v_{ij} \frac{k_i}{k} T_k, \tag{3.9}$$

with

$$v_{ij} = \langle \tau^{\frac{1}{2}} \rangle \delta_{ij} + \left\langle \frac{\tau_i \tau_j}{\tau^{\frac{3}{2}}} \right\rangle = \langle t \rangle \delta_{ij} + \left\langle \frac{t_i t_j}{t} \right\rangle.$$

In (3.9) summation over repeated indices is implied. The off-diagonal elements of the tensor v_{ij} are zero in the coordinate system with $\sigma_{12} = 0$; the diagonal elements are given by

$$\left.\begin{aligned} v_{11} &= \left\langle t + \frac{t_1^2}{t} \right\rangle = \sigma_{11}^{\frac{1}{2}} \tfrac{3}{4}(2\pi)^{\frac{1}{2}} F(-\tfrac{1}{2}, \tfrac{1}{2}, 2, A) =: \sigma_{11}^{\frac{1}{2}} F_1(A) \\ v_{22} &= \left\langle t + \frac{t_2^2}{t} \right\rangle = \sigma_{11}^{\frac{1}{2}} \tfrac{3}{4}(2\pi)^{\frac{1}{2}} F(-\tfrac{1}{2}, \tfrac{3}{2}, 2, A) =: \sigma_{11}^{\frac{1}{2}} F_2(A), \end{aligned}\right\} \tag{3.10}$$

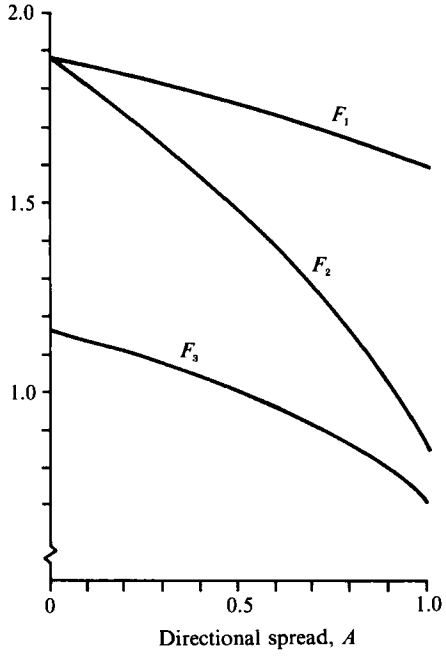

FIGURE 2. F_1, F_2 and F_3 as functions of the directional spread $A, 0 \leqslant A \leqslant 1$ by definition, see equations (3.7) and (3.10).

with F and A as above. The functions F_1, F_2 and F_3 are depicted in figure 2. It is clear from (3.7) and (3.10) that v_{11} and v_{22} are proportional to the average friction velocity $\langle \tau_0^{\frac{1}{2}} \rangle$, with proportionality factors which depend on the directional spread A.

Finally

$$\frac{\boldsymbol{k}}{k} \cdot \left\langle \frac{\partial}{\partial \tilde{U}_k} \boldsymbol{\tau} \right\rangle = v_{ij} \frac{k_i k_j}{k^2} T_k$$

$$= \sigma_{11}^{\frac{1}{2}} \{F_1(A) \cos^2(\tilde{\theta}) + F_2(A) \sin^2(\tilde{\theta})\} T_k \tag{3.11}$$

where $\tilde{\theta}$ is the angle between the wave direction and the main axis of the bottom stress spectrum.

3.3. *A characteristic scale for the turbulent velocity*

Comparing (3.11) with (3.8) one finds that the factor $\langle \tau_0^{\frac{1}{2}} \rangle$, which appears in the linear formulation, is replaced by $v_{ij} k_i k_j / k^2$ in the nonlinear formulation. Denote this factor by v_t:

$$\frac{\boldsymbol{k}}{k} \cdot \left\langle \frac{\partial}{\partial \tilde{U}_k} \boldsymbol{\tau} \right\rangle = v_t T_k. \tag{3.12}$$

Substituting this expression in (2.19) it is found that

$$\tau_i = \sum_{\boldsymbol{k}} v_t(\boldsymbol{\tau}, \boldsymbol{k}) T_k \frac{k_i}{k} \tilde{U}_k + \text{c.c.} \tag{3.13}$$

It follows that v_t, which has the dimension of a velocity, characterizes the intensity of the first-harmonic stress components. Only these contribute to the energy dissipation, so that v_t characterizes the intensity of the stress, as it works on the mean flow. In the linear case the first harmonics (3.13) equal the definition (3.1a); v_t

depends on the stress only. In the nonlinear case (3.13) represents that part of the stress, which contributes to the energy dissipation. The nonlinear v_t depends on the stress, as well as on the direction relative to the stress of the wavenumber $\boldsymbol{k}$.

Note that (3.13) parameterizes $\tau_i = \delta\tau_i^1$, whereas τ_i^1 was considered in §2. The choice of the (average) friction velocity as a velocity scale implicitly defines the expansion parameter δ. Combining (3.13) with (2.12) the parameter δ is identified as

$$\delta = v_t k/\omega. \tag{3.14}$$

The scale for the boundary-layer thickness is thus found as v_t/ω, which has to be small compared to a wavelength as stated earlier.

The velocity v_t is itself again a function of δ: the variances σ_{11} and σ_{22}, which define v_t according to (3.8) and (3.11), depend on δ through the function $T_k(z_0)$, which occurs in (3.5). Given a surface elevation spectrum $F(\boldsymbol{k})$, a water depth h and a bottom roughness k_N, σ_{11} and σ_{22} are implicitly defined by (3.5). They have to be determined iteratively. It can be proved that the iteration converges to a unique solution, if $\sigma_{11}^{\frac{1}{2}}$ and $\sigma_{22}^{\frac{1}{2}}$ are slowly varying functions of z_0 (Weber 1989). This condition implies that the iterative scheme cannot depend sensitively on the bottom roughness and therefore v_t itself cannot depend sensitively on k_N.

3.4. *The energy dissipation*

The energy dissipation can now be determined from (2.20) and (3.12). Rewriting the slow time derivative in terms of the original variable t, one finds

$$\frac{\partial}{\partial t}F(\boldsymbol{k}) = -\{T_k(z_0)+\text{c.c.}\}\frac{v_t k}{\sinh 2kh}F(\boldsymbol{k}), \tag{3.15}$$

with v_t defined as

$$v_t = \sigma_{11}^{\frac{1}{2}}F_3(A) \qquad \text{(linear)}, \tag{3.16a}$$

$$v_t = \sigma_{11}^{\frac{1}{2}}\{F_1(A)\cos^2(\tilde{\theta})+F_2(A)\sin^2(\tilde{\theta})\} \quad \text{(nonlinear)}. \tag{3.16b}$$

Note that the energy dissipation depends on δ through the timescale $(v_t k)^{-1}$, as well as through the lengthscale in $z_0 = k_N/(30\delta)$. Since δ has to be small, the dissipation timescale has to be large compared to a wave period.

For later use I will define a dissipation coefficient C as

$$C = v_t\{T_k(z_0)+T_k^*(z_0)\}. \tag{3.17}$$

C has the dimension of a velocity. The dissipation coefficient depends on the spectrum through the characteristic velocity v_t.

A linear or a nonliner parameterization of the bottom stress results in the same basic expression (3.15) for the energy dissipation. The word 'nonlinear' is misleading in this context, as it is the linearized stress which determines the dissipation. The nonlinearity of the stress parameterization only shows up in the form of v_t. Comparing (3.16*a*) and (3.16*b*) there are two outstanding differences:

(i) the nonlinear v_t depends on the direction of a wave component, while the linear v_t is isotropic;

(ii) v_t is determined from different iteration schemes, because of the different definitions (3.16*a*) and (3.16*b*).

To illustrate the second point, consider the one-dimensional limit $A = 1$, which occurs for a one-dimensional surface elevation spectrum. In the linear case v_t is determined from

$$v_t = F_3(1)\,[\sigma_{11}(v_t)]^{\frac{1}{2}}.$$

In the nonlinear case v_t is determined from

$$v_t = F_1(1)\,[\sigma_{11}(v_t)]^{\frac{1}{2}}.$$

The ratio between the linear and the nonlinear velocities v_t depends on the actual spectrum, water depth and bottom roughness, but is likely to be smaller than one. Turning the argument around: suppose a given spectrum $F(\boldsymbol{k})$ would induce a turbulent velocity v_t according to the nonlinear parameterization. A spectrum $\tilde{F}(\boldsymbol{k})$, given by $[F_1(1)/F_3(1)]^2 F(\boldsymbol{k}) \approx 6F(\boldsymbol{k})$ (see figure 2), would then induce the same velocity in the linear parametrization. The spectrum $\tilde{F}$ corresponds to a significant wave height, which is 2.5 times the significant wave height found with the spectrum F. The dissipation rate is thus expected to be larger in the case of a nonliner parameterization, for a given wave spectrum, water depth and bottom roughness.

4. Examples of the generalized parameterization

The linear eddy-viscosity model and the quadratic drag law are examples of a linear and a nonlinear parameterization respectively. The eddy-viscosity model parameterizes the stress in the boundary layer. This implies that the stress and velocity profiles in the bottom boundary layer can be computed as well as the energy dissipation. The drag law parameterizes the bottom stress and yields only the energy dissipation. Two eddy-viscosity models will be discussed: one developed by the author and the other given recently by Madsen *et al.* (1989). The different forms of the eddy-viscosity and the drag-law dissipation functions can be explained from the results of §3.

4.1. *A spectral eddy-viscosity model*

In the eddy-viscosity model the turbulent stress is related to the vertical gradient of the velocity through an eddy-viscosity coefficient ϵ:

$$\tau_i(z) = \epsilon \frac{\partial u_i}{\partial z}. \tag{4.1}$$

A one-layer model is used here: $\epsilon = \kappa u^* z$ throughout the boundary layer, with $\kappa = 0.4$ the von Kármán constant and $u^* = \langle \tau_0^{\frac{1}{2}} \rangle$.

According to (4.1) the stress and the stream function are related through

$$\delta\tau_1^1 = -\kappa u^* z \psi_{2zz}^1, \qquad \delta\tau_2^1 = \kappa u^* z \psi_{1zz}^1. \tag{4.2}$$

From (4.2) and the boundary-layer equations (2.6*a*) $\boldsymbol{\tau}^1$ and $\boldsymbol{\psi}^1$ can be determined. This will be done in terms of T_k; using (2.10), (2.12) and (3.13) (with $v_t = u^*$) it follows that

$$T_{kzz}^* - \frac{\mathrm{i}}{\kappa}\frac{1}{z} T_k^* = 0. \tag{4.3}$$

The boundary conditions are as given in (2.11). From Abramowitz & Stegun (1965, ch. 9) the solution can be determined in terms of Bessel functions of integer order, for example in terms of the zero-order Kelvin function $\mathrm{Ker} + \mathrm{i}\,\mathrm{Kei}$, as

$$T_k^* = -\tfrac{1}{2}\kappa\xi \frac{\mathrm{Ker}'(\xi) + \mathrm{i}\,\mathrm{Kei}'(\xi)}{\mathrm{Ker}_0(\xi_0) + \mathrm{i}\,\mathrm{Kei}_0(\xi_0)}, \tag{4.4}$$

with argument $\xi = [4kz/\kappa]^{\frac{1}{2}}$. Here the prime denotes the derivative with respect to ξ and the subscript zero for ξ denotes the value in $z = z_0$. The bottom stress components are thus related to the free-stream velocity components according to

$$\tilde{\tau}_k(z_0) = u^* T_k(z_0)\,\tilde{U}_k, \tag{4.5}$$

with T_κ as given above.

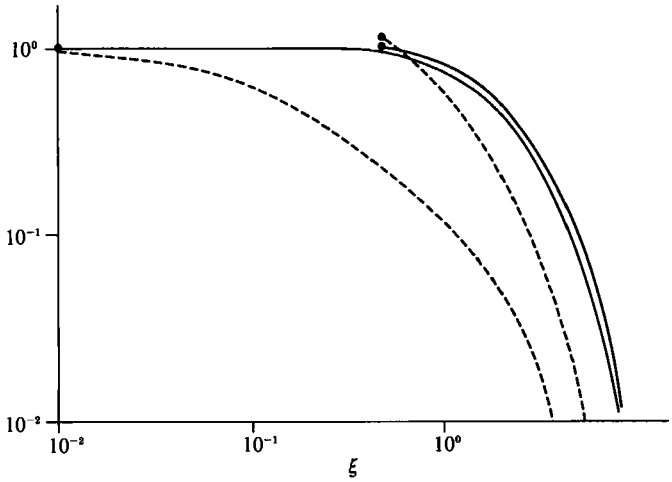

FIGURE 3. The modulus τ_k of the stress components and the modulus $U_k - u_k$ of the defect velocity components, made dimensionless with their value at the bottom, as a function of the dimensionless height ξ, for example roughness lengths $\xi_0 = 0.01$ and $\xi_0 = 0.5$. Solid line, stress; dashed line, defect velocity.

The boundary layer is defined as the layer where the velocity deviates significantly from the free-stream velocity. The thickness of the boundary layer is determined by the decay with height of the so-called defect velocity (the free-stream velocity minus the boundary-layer velocity). The modulus of the defect velocity and of the stress, normalized by their value at the bottom, are given in figure 3 for two example bottom roughness lengths. It is clear that for $\xi \approx 7$ the defect velocity deviation is less than 1 % and the stress is less than 3 % of its bottom value (this holds for scaled roughness lengths ξ_0 up to about 1). A height $\xi \approx 7$ corresponds to $(y+h) \sim 5l$, with $l = u^*/\omega$ and $A = 0.7$. Therefore the boundary-layer thickness can be taken as $d \sim 5l$.

From general dimensional arguments an inertial sublayer with a logarithmic velocity profile is expected, if there is a range of distances $y+h$ such that $(y+h)/k_N \gg 1$ and $(y+h)/d \ll 1$ simultaneously (Tennekes & Lumley 1972). This is only possible if $k_N/d \ll 1$ or, equivalently, if $\xi_0 \ll 1$. The eddy-viscosity parameterization then allows for an inertial sublayer, as in the limit for small arguments the velocity profile is logarithmic and the stress is constant with height.

The energy dissipation is given by (3.15) as

$$\frac{\partial}{\partial t} F(\boldsymbol{k}) = u^* \{T_k(\xi_0) + T_k^*(\xi_0)\} \frac{k}{\sinh 2kh} F(\boldsymbol{k}), \tag{4.6}$$

with T_k now defined in (4.4). The parameterization (4.5) allows for a phase shift ζ_k between a bottom stress component and a free-stream velocity component, because T_k is complex. A phase shift diminishes the energy dissipation through the factor $T_k + T_k^* = 2(T_k T_k^*)^{\frac{1}{2}} \cos(\zeta_k)$. In figure 4 the functions $T_k + T_k^*$ and $T_k T_k^*$ are given. The energy dissipation depends nonlinearly on the bottom velocity spectrum and the bottom roughness through the friction velocity u^*, which is determined from $u^* = \sigma_{11}^{\frac{1}{2}} F_3(A)$, with the variances σ_{11} and σ_{22} defined by (3.5).

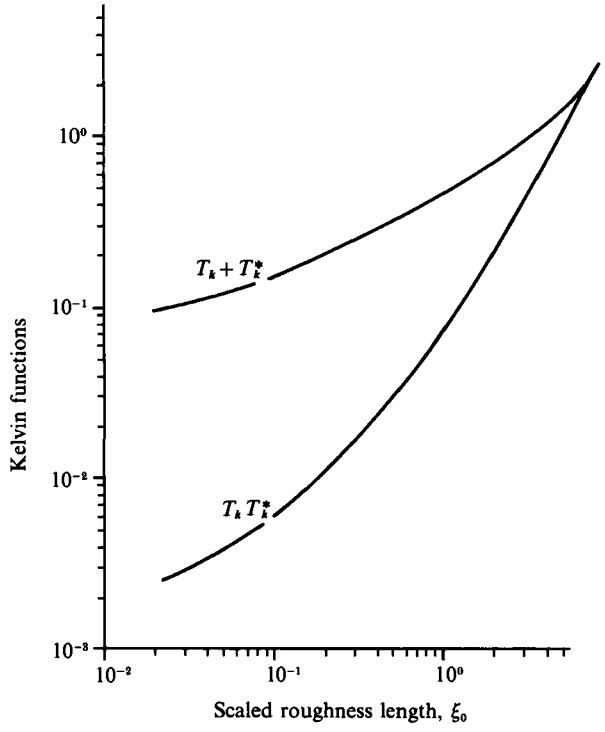

FIGURE 4. The spectral energy dissipation (4.6) is proportional to $T_k(\xi_0)+T_k^*(\xi_0)$ and to the average friction velocity u^*, which is determined from $T_k(\xi_0)\,T_k^*(\xi_0)$.

4.2. *A spectral model using a representative monochromatic wave*

Recently Madsen *et al.* (1989) have presented an eddy-viscosity model for the random wave case. They also use a one-layer model, but with a different definition for the friction velocity: $u^* = \langle 2\tau_0^2\rangle^{\frac{1}{4}}$. With this definition the friction velocity depends on the total stress only and not on the directional distribution of the stress spectrum. Strictly speaking this model does not comply with the definition (3.1*a*), but it does fall in the class of linear parameterizations and the results of §3 apply. For a given directional distribution, $\langle 2\tau_0^2\rangle^{\frac{1}{4}}$ is proportional to and larger than $\langle \tau_0^{\frac{1}{2}}\rangle$.

Solving the boundary-layer equations, Madsen *et al.* arrive at an expression for the bottom stress similar to (4.5) with (4.4). Two approximations are then made:

(i) a logarithmic approximation for the Kelvin function, which is only valid for $\xi_0 \ll 1$ (Madsen *et al.* 1989);

(ii) the wavenumber in T_k is replaced by a 'representative' wavenumber.

The second approximation makes it possible to write the friction velocity as

$$u^* = (T_k\,T_k^*)^{\frac{1}{2}}\langle 2U^2\rangle^{\frac{1}{2}} =: c_{\mathrm{DM}}^{\frac{1}{2}}\langle 2U^2\rangle^{\frac{1}{2}}, \tag{4.7}$$

with $U = (U_1^2+U_2^2)^{\frac{1}{2}}$. Neglecting subsequently the phase shift between the bottom stress and the free-stream velocity, which is again only allowed for small ξ_0, it is found that

$$\frac{\partial}{\partial t}F(\boldsymbol{k}) = -2c_{\mathrm{DM}}\langle 2U^2\rangle^{\frac{1}{2}}\frac{k}{\sinh 2kh}F(\boldsymbol{k}). \tag{4.8}$$

Apart from a factor $\sqrt{2}$ this is Collins' expression for the energy dissipation due to bottom friction (see §4.3). The coefficient c_{DM} can be computed numerically or an experimentally determined expression can be used.

This model differs from the one presented in §4.1 primarily in the approximations which are made to obtain (4.8). The neglect of the wavenumber dependency of the function T_k will be discussed in §4.4. The first approximation is valid for small values of the scaled roughness ξ_0, which are associated with a flat sea bed. This occurs when the orbital bottom velocity U is small and there are no tide-generated sand ripples. Evidently, U should not be so small that the boundary layer is no longer fully turbulent. However, a scaled roughness of the order 0.01 yields a dissipation rate which is negligible compared to other mechanisms which are important for ocean waves, like the wind input or dissipation by whitecapping (Weber 1991).

4.3. *The drag law*

In the quadratic drag law the bottom stress is parameterized as

$$\tau_i(z_0) = c_{\mathrm{D}} U U_i. \tag{4.9}$$

For monochromatic rough turbulent flows c_{D} has been determined experimentally as a function of $k_{\mathrm{N}}\omega/U$ (see for example Jonsson 1980).

As $\tau_0^{\frac{1}{2}} = c_{\mathrm{D}}^{\frac{1}{2}} U$, the drag law can be considered as a degenerate case of (3.1*b*), with $T_k = c_{\mathrm{D}}^{\frac{1}{2}}$ and $t_i = c_{\mathrm{D}}^{\frac{1}{2}} U_i$ $(i = 1, 2)$. This implies that $\sigma_{it} = \langle t_i^2 \rangle = c_{\mathrm{D}} \langle U_i^2 \rangle$. The characteristic velocity v_{t} is found from (3.16*b*) as

$$v_{\mathrm{t}} = c_{\mathrm{D}}^{\frac{1}{2}} \langle U_1^2 \rangle^{\frac{1}{2}} \{F_1(A) \cos^2(\tilde{\theta}) + F_2(A) \sin^2(\tilde{\theta})\}, \tag{4.10}$$

with $A = 1 - \langle U_2^2 \rangle / \langle U_1^2 \rangle$. The linearized form of (4.9), which effectively determines the energy dissipation, now follows from (3.13) as

$$\tau_i(z_0) = c_{\mathrm{D}}^{\frac{1}{2}} v_{\mathrm{t}} U_i, \tag{4.11}$$

with v_{t} as defined in (4.10). The energy dissipation is given by

$$\frac{\partial}{\partial t} F(\boldsymbol{k}) = -2 c_{\mathrm{D}}^{\frac{1}{2}} v_{\mathrm{t}} \frac{k}{\sinh 2kh} F(\boldsymbol{k}). \tag{4.12}$$

This expression is equivalent to the one given by Hasselmann & Collins (1968). From a limited number of numerical hindcasts they estimated $c_{\mathrm{D}} = 0.015$. Note that this value applies to the first harmonics of the stress (4.11) and to the energy dissipation (4.12), but not to the original drag law (4.9). The use of a constant drag coefficient is probably not adequate for wave forecasts, taking into account the range of $k_{\mathrm{N}}\omega/U$ values which can occur for storm waves in shallow water (Shemdin *et al.* 1978).

Collins (1972) proposed to approximate the energy dissipation (4.12) by replacing the characteristic velocity (4.10) by $v_{\mathrm{t}} = c_{\mathrm{D}}^{\frac{1}{2}} \langle U^2 \rangle^{\frac{1}{2}}$, which corresponds to a drag law $\tau_i(z_0) = c_{\mathrm{D}} \langle U^2 \rangle^{\frac{1}{2}} U_i$. This 'approximation' is essentially an alternative formulation of the drag law for a random wave field, as this relation cannot be derived from the drag law (4.9) used by Hasselmann & Collins.

4.4. *Comparison*

4.4.1. *Spectral versus 'monochromatic' approach*

Under stationary and homogeneous wind conditions an initial wave spectrum develops until saturation is reached. The spectral shape is preserved during the evolution, owing to third-order wave–wave interactions. The total energy increases and the energy-containing range of the spectrum shifts to lower frequencies, because of the transfer of energy by the resonant interactions. Equilibrium is attained when

the sum of the wind input, the dissipation by whitecapping and the nonlinear energy transfer is zero over the whole spectral range (JONSWAP 1973). In shallow water the influence of the bottom is felt as soon as the wave-induced bottom velocity has become large enough to give rise to a bottom boundary layer. Equilibrium is reached in an earlier stage than in deep water, because of the additional dissipation due to bottom friction. The evolution depends crucially on the balance on the low-frequency face of the spectrum between the input of energy by the nonlinear transfer and the dissipation by bottom friction (Weber 1988).

Under these idealized circumstances the spectrum is self-similar. It can be represented by one parameter, which basically denotes the state of development of the wave field. Moreover, the bottom velocity spectrum is initially narrow. For such spectra the wavenumber in T_k can be replaced by a representative wavenumber. The wave component with maximum energy gives a good representation (Weber 1991) and the second approximation made by Madsen *et al.* is fully justified for these cases. In very shallow water the bottom velocity spectrum is broader, because more wave components extend down to the sea floor. In figure 5(*a*) an example is given of the variation of the coefficient C (defined in (3.17)) over the energy-containing spectral range. The value which is found using the peak wavenumber is also indicated. A 'monochromatic' approach is thus seen to overestimate the dissipation at lower frequencies and to underestimate the dissipation at higher frequencies. In the evolution of the spectrum this could be significant, in view of the role bottom dissipation and the nonlinear transfer play on the forward face of the spectrum.

In realistic situations the wind field is often inhomogeneous and changeable. The spectral evolution is not so straightforward then as sketched above. The spectrum loses its self-similar form and double peaks can appear. Examples are swell interacting with wind–sea or waves generated by a fast-turning wind field. In the case of swell, the dissipation would be largely overestimated by the use of the wavenumber with maximum energy, see figure 5(*b*). This is usually the peak of the wind–sea spectrum. When there is a sudden shift in the wind direction, a new wave spectrum develops in the new wind direction. It is not possible to define a representative wavenumber during the transformation from the old to the new wind direction. In some of these cases a representative wavenumber can possibly be defined from the bottom velocity spectrum, taking into account the actual variation in the Kelvin functions in the spectral formulation. In other cases a full spectral approach has to be used. A further evaluation of the importance of spectral effects has to come from numerical experiments (with explicit calculations of the resonant four-wave interactions) or from field measurements.

4.4.2. *Eddy-viscosity model versus the drag law*

The eddy-viscosity model and the drag law differ firstly in the function which relates the bottom stress to the free-stream velocity. In the eddy-viscosity model T_k is defined by (4.4). It is complex and hence allows for a phase shift. In the drag law T_k is given as $c_{\mathrm{D}}^{\frac{1}{2}}$; the wavenumber dependency and the phase shift are neglected *a priori*. The drag coefficient is often taken as constant or an expression is used which has been determined experimentally for monochromatic waves. In the latter case a representative wave has to be determined from the random wave field, which is not necessarily possible. The eddy-viscosity dissipation and the drag law can be reconciled partly by defining the drag coefficient as $c_{\mathrm{D}}^{\frac{1}{2}} = T_k$, with T_k defined by (4.4). This introduces a phase shift in the first-harmonics part (4.11) of the drag law. The drag-law expression and the eddy-viscosity expression would then depend in a

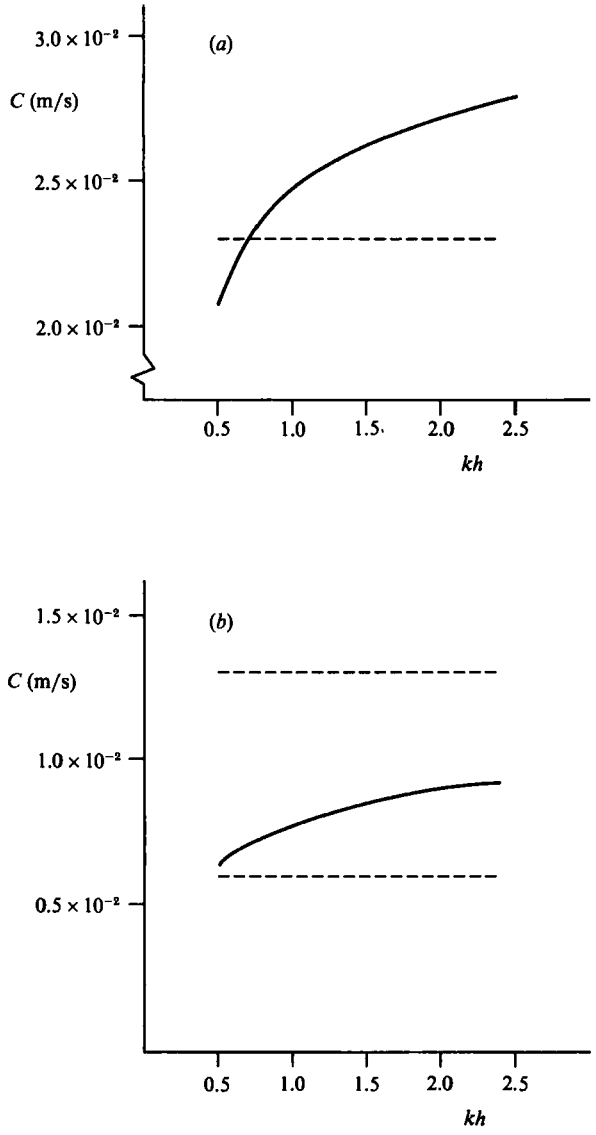

FIGURE 5. (*a*) The coefficient C as a function of non-dimensional wavenumber kh for an example single-peaked spectrum with a significant wave height of 6.5 m and a peak frequency of 0.09 Hz in 15 m water depth. The non-dimensional peak wavenumber is $k_p h = 0.8$. Solid line, the spectral eddy-viscosity model; dashed line, monochromatic approximation. (*b*) As in (*a*) but now for an example double-peaked spectrum with a significant wave height of 2.0 m and peaks at 0.3 and 0.06 Hz in 15 m water depth. The wave height, which can be associated with the swell, is 0.8 m. The non-dimensional peak wavenumbers are $k_p h = 0.5$ and $k_p h = 6.0$. (Bottom dissipation is relevant for $kh < 2.5$). Solid line: the spectral eddy-viscosity model. Upper dashed line, monochromatic approximation using the wind–sea peak; lower dashed line, monochromatic approximation using the swell peak.

similar way on the scaled bottom roughness. The drag-law dissipation would however be stronger due to the functions F_1 and F_2 which occur in (4.10). These take larger values than the function F_3 which occurs in the linear formulation.

The second point is the different phase dependency of the two parameterizations.

	H_s (m)	$k_p h$	f_p (Hz)	$\langle U^2 \rangle^{\frac{1}{2}}$ (m/s)
Texel	7	1.1	0.086	0.60
Euro	5	1.4	0.110	0.45

TABLE 1. Wave parameters for the stations Texel (depth $h = 30$ m) and Euro (depth $h = 25$ m) on 3 January 1976. The spectra have an angular distribution with $A = 0.7$. The equilibrium values of the significant wave height H_s, the non-dimensional water depth $k_p h$, the peak frequency f_p and the r.m.s. bottom velocity $\langle U^2 \rangle^{\frac{1}{2}}$ are given.

In the eddy-viscosity model the relation (4.5) between the bottom stress and the free-stream velocity is linear in the random wave phase. The characteristic velocity u^* is isotropic. The drag law (4.9) is nonlinear in the random wave phase. The characteristic velocity (4.10) therefore depends on the direction of a wave component.

For stationary flows the eddy-viscosity concept and the drag law are compatible. Extension of these models to oscillatory flows introduces a phase shift, which has to be included in the drag law in order to reconcile the two models. In the random wave case a reconciliation is only possible if the first harmonics of the drag law are considered. The nonlinear formulation (4.9) is basically incompatible with the linear eddy-viscosity parameterization (4.5).

4.5. *Applications*

Two examples will now be given to illustrate the different models. The examples are taken from a severe depth-limited storm which occurred in the southern North Sea on 3 January 1976. This storm has been analysed by Bouws & Komen (1983) and Weber (1991). There are measurements of the wave spectrum from two stations off the Dutch coast, about 200 km apart. At both stations an equilibrium was established, which persisted for about 12 h. Some parameters for the equilibrium wave fields are given in table 1.

The local change in the wave spectrum is given by the balance between wind input, dissipation at the surface and at the bottom, the transfer of energy within the spectrum by resonant wave–wave interactions and the advection of energy by propagation. The terms in the energy balance can be computed from the measured data. During the equilibrium phase of the storm the local change is zero: a value for C which minimizes the local change thus adequately represents the equilibrium phase of the storm. This yields $C = 0.014$ m/s for the station Texel and $C = 0.015$ m/s for the station Euro. The errors in this estimate are determined by the state of the art in wave modelling (WAMDI group 1988). These values correspond to a local change in the spectrum, which is two orders of magnitude smaller than the individual sources and sinks. This gives some weight to the reliability of the estimate.

The dissipation coefficient C can also be computed directly from the eddy-viscosity model, using the measured data. A value is needed for the roughness length in order to do this. In Weber (1991) it is proposed that a constant roughness value ($k_N = 4$ cm) is used and then check *a posteriori* whether this value is consistent with the flow conditions. The ripple regimes for the two stations were estimated from the local bed material. It was found that the bed is flat for $U < 15$ cm/s, whereas sheet flow occurs for $U > 70$ cm/s. In the former case the roughness is given by the sand grain diameter, in the latter it is determined by the flow itself (Wilson 1989). In the intermediate range ripples are present and the roughness scales with the ripple height. During the equilibrium phase of the storm U is 60 cm/s at Texel and 45 cm/s

at Euro. This corresponds to so-called transition ripples, with a steepness of about 0.1 and a ripple height of 1–2 cm. This is consistent with the proposed roughness value.

According to the linear eddy-viscosity model the friction velcoity $v_t = u^*$ follows from (3.16*a*), (3.5) and (4.4), with $F(\boldsymbol{k})$ as measured during the equilibrium phase of the storm. The computation converges for both stations within ten iterations, with $u^* = 6$ cm/s (Texel) and $u^* = 5$ cm/s (Euro) respectively. The ratio $k_N u^*/\nu$ between the roughness length and the thickness of the viscous sublayer is of the order 10^3, which means that the flow is indeed fully rough turbulent. The expansion parameter δ is 0.004 for both stations. This yields a boundary-layer thickness $d = 5u^*/\omega$ of 55 cm (Texel) and 35 cm (Euro). Wavelengths range from 100–200 m. The Reynolds number $R = Ud/\nu$ is of the order 10^5. The values found for $k_N u^*/\nu$, δ and R show that the assumptions made to derive the bottom dissipation expression are justified for the applications considered here. From the computed values for the friction velocity and the scaled bottom roughness ($\xi_0 = 0.4$) the coefficient C (for the peak frequency) can be determined using (4.4) and (3.17). This yields $C = 0.016$ m/s (Texel) and $C = 0.015$ m/s (Euro), which is quite close to the values estimated from the data.

The eddy-viscosity model by Madsen *et al.* is formulated in terms of a drag coefficient. Taking the option to determine this coefficient from the data it follows that for Texel $c_{DM} = 0.008$ and for Euro $c_{DM} = 0.012$. The Hasselmann & Collins expression depends on the direction of a wave component relative to the main axis of the bottom velocity spectrum. For the main direction a drag coefficient $c_D = c_{DM}$ would fit the data. The value $c_D = 0.015$ would yield a dissipation rate which is much too high. Computing the drag coefficient from Jonsson (1980), who gives an experimentally determined expression in terms of the parameter $\sqrt{2}U/k_N\omega$, one finds $c_D = 0.015$ for Texel and $c_D = 0.020$ for Euro. (These values are larger than the ones determined from the data, because of the hypergeometric functions in (4.12) and the factor $\sqrt{2}$ in (4.8).)

The two examples considered here demonstrate that the coefficient C can be computed with the roughness length fixed. This seems a better option than to fix the drag coefficient, as proposed by Hasselmann & Collins. There is no indication that a nonlinear parameterization yields a better estimate of the spectral energy dissipation due to bottom friction than a linear parameterization. As the data are obtained under equilibrium conditions, it is to be expected that there is no significant difference between a spectral description and a description in terms of the peak frequency. This is indeed the case if the drag coefficient c_{DM} is estimated from the storm data. If an experimentally determined expression is used for the drag coefficient in the 'monochromatic' eddy-viscosity model, the dissipation rate is much too high. The close agreement between the values for C computed from the eddy-viscosity model and the values estimated from the storm data suggests that this model can be successfully applied in wave modelling.

5. Summary and conclusions

The energy dissipation of random ocean waves due to friction in the turbulent bottom boundary layer has been computed, using an expansion in the parameter δ. Here δ denotes the ratio between the boundary-layer thickness and a wavelength. The turbulent stress retards the flow near the bottom and thereby induces order-δ modifications in the pressure and the velocity above the boundary layer. These work their way up through the water column and finally modify the surface elevation. The

modifications are determined by the bottom stress and the wave phase velocity; they fall off exponentially away from the bottom. The spectral energy dissipation can therefore be expressed in terms of the bottom stress and the free-stream bottom velocity. This result is valid at first order in wave steepness, under the assumptions that δ is small, that the flow is fully rough turbulent and that the stress can be parameterized in terms of the free-stream bottom velocity.

The boundary-layer equations suggest a certain form of stress parameterization. This basic form is used in the next step, with the average or the instantaneous friction velocity as the velocity scale. The resulting two formal parameterizations are used to investigate the dependence of the dissipation expression on the stochastic characteristics of the stress. It was found that a linear parameterization (average friction velocity) yields a dissipation coefficient which is isotropic. A nonlinear parameterization (instantaneous friction velocity) yields a directionally dependent dissipation coefficient. The dissipation rate is stronger in the case of a nonlinear parameterization than in the case of a linear one.

One dissipation expression developed by the author and three expressions existing in the literature are discussed within the framework of the formal theory. The models discussed are: a linear eddy-viscosity model developed by the author for random ocean waves, an eddy-viscosity model given by Madsen *et al.* based on an 'equivalent' monochromatic wave (1989), the drag law as used by Hasselmann & Collins (1968) and an approximation to this drag-law expression given by Collins (1972).

The model by Madsen *et al.* differs in a number of respects from the model developed by the author; most importantly, it approximates the random wave field by an 'equivalent' monochromatic wave instead of retaining a spectral description. A spectral approach and a monochromatic approach are equivalent for narrow and single-peaked bottom velocity spectra. These occur under homogeneous and stationary wind conditions, in moderately shallow water. In extremely shallow water the bottom velocity spectrum is broader. If the wind field is inhomogeneous and changeable the spectrum loses its self-similar form, so that there is no representative wavenumber. Examples are swell interacting with wind–sea or waves generated by a fast-turning wind field. For most of these cases a full spectral model has to be used.

The eddy-viscosity model is linear in the random wave phase, whereas the drag law is nonlinear. This explains the differences between the eddy-viscosity expressions and the Hasselmann & Collins expression. The dissipation coefficient is isotropic in the case of the eddy-viscosity model, whereas it is directionally dependent in the Hasselmann & Collins expresion. (Collins approximates this expression by leaving out the directional dependency.) The drag law relates the dissipation rate to the non-dimensional bottom roughness by means of a drag coefficient, which has to be determined experimentally. This relation is computed from the stress parameterization in the eddy-viscosity model. The two models can be partly reconciled by defining the drag coefficient to be equal to the analogous function in the eddy-viscosity model.

The eddy-viscosity model agrees rather well with data from two cases of storm waves in shallow water. There is no indication in these examples that a nonlinear parameterization performs better than a linear one. It is proposed that a fixed roughness length is used in the eddy-viscosity model. This seems a better option than a fixed drag coefficient as proposed by Hasselmann & Collins. The eddy-viscosity model is self-contained, but takes about 30 % more computing time than the drag law because of the iterative determination of the friction velocity. The iteration is

convergent, on the condition that the friction velocity does not depend strongly on the roughness length. This justifies the assumption of a fixed roughness length, whereas in reality ripples grow and decay dynamically with the wave field. The computation converges in practice within ten iterations.

A rough test of the different models is to implement the dissipation expressions in a shallow-water wave model and to compare the model performance with wave measurements. The validation then depends on how accurately other physical processes are represented in the wave model. Hindcasts of an extreme storm and a case of swell in a depth-limited sea are discussed in Weber (1991).

Direct validation could be done using measurements of the turbulent bottom stress, or of the boundary-induced order-δ pressure fluctuations above the wave boundary layer. This is up till now impossible, because of the scarcity of field or laboratory data on the random wave boundary layer. Recently there have been a number of experiments on continental shelves in combined wave–current situations, see Huntley & Hazen (1988) for an overview. Unfortunately all measurements are taken well above the wave boundary layer. Moreover, in all of these experiments the random wave field is reduced to a representative monochromatic wave, although Huntley & Hazen point out the difficulties in selecting a representative wave direction, frequency and amplitude. Hopefully, this study provides a basis for future modelling and measurments which take the randomness of the wave field into account.

I would like to thank Sjef Zimmerman, Gerbrand Komen and Aad van Ulden for valuable discussions. Greet de Graaf-Boshuis is thanked for typing the various versions of the manuscript. Financial support was provided by the research community Meteorology and Physical Oceanography (MFO) of the Netherlands Organisation for Scientific Research (NWO).

Appendix

In this Appendix all results related to ensemble averaging, which are needed in §3, are derived.

A.1. *Horizontal coordinate system*

The horizontal coordinate system at $z = z_0$ can always be chosen such that $\sigma_{12} = 0$. If t_1 and t_2 are jointly Gaussian, their joint distribution function is

$$f(\boldsymbol{t}) = \frac{1}{(2\pi D)^{\frac{1}{2}}} \exp\left[-\tfrac{1}{2}({}^{\mathrm{T}}\boldsymbol{t}\boldsymbol{\Lambda}^{-1}\boldsymbol{t})\right]$$

with

$$D = \tilde{\sigma}_{11}\tilde{\sigma}_{22} - \tilde{\sigma}_{12}^2, \quad \boldsymbol{\Lambda}^{-1} = \frac{1}{D}\begin{pmatrix} \tilde{\sigma}_{22} & -\tilde{\sigma}_{12} \\ -\tilde{\sigma}_{12} & \tilde{\sigma}_{11} \end{pmatrix}.$$

The tildes denotes values with respect to the original coordinate system. As $\boldsymbol{\Lambda}^{-1}$ is symmetric, there exists a real unitary matrix $\boldsymbol{U}$ such that ${}^{\mathrm{T}}\boldsymbol{U}\boldsymbol{\Lambda}^{-1}\boldsymbol{U}$ is a diagonal matrix. Straightforward algebra shows that $\boldsymbol{U}$ is a rotation through ϕ, with ϕ defined by

$$\phi = \tfrac{1}{2}\arctan\left(2\tilde{\sigma}_{12}/(\tilde{\sigma}_{11} - \tilde{\sigma}_{22})\right)$$

and

$${}^{\mathrm{T}}\boldsymbol{U}\boldsymbol{\Lambda}^{-1}\boldsymbol{U} = \begin{pmatrix} 1/\sigma_{11} & 0 \\ 0 & 1/\sigma_{22} \end{pmatrix},$$

where σ_{11} and σ_{22} are relative to the rotated coordinate system.

$\sigma_{22} \leqslant \sigma_{11}$ can always be achieved by interchanging the role of the x_1- and x_2-axes. The coordinate system which has $\sigma_{12} = 0$ then yields the maximum value for σ_{11} and the minimum value for σ_{22}, as compared to all other possible coordinate systems.

A surface elevation spectrum, which has an axis of symmetry, always has $\sigma_{12} = 0$ in a coordinate system with the axis of symmetry as the x_1-axis. This follows from the definition (3.5) of σ_{12}:

$$\sigma_{12} = \langle t_1 t_2 \rangle = \int_{k,\theta} k(T_k T_k^*) \frac{\omega^2}{\sinh^2 kh} [\cos\theta \sin\theta \, F(k,\theta) \, \mathrm{d}\theta] \, \mathrm{d}k = 0.$$

A.2. *Derivatives of the bottom stress*

If τ_i is linear

$$\left\langle \frac{\partial}{\partial \tilde{U}_k} \tau_i \right\rangle = \langle \tau^{\frac{1}{2}} \rangle \frac{k_i}{k} T_k = \langle t^{\frac{1}{2}} \rangle^2 \frac{k_i}{k} T_k.$$

On the other hand, if τ_i is nonlinear, it follows from the definition (3.1*b*) of τ_i and the definition of $\tau^{\frac{1}{2}}$ that

$$\frac{\partial}{\partial \tilde{U}_k} \tau^{\frac{1}{2}} = \frac{\tau_1}{\tau} \frac{\partial}{\partial \tilde{U}_k} \frac{\tau_1}{\tau^{\frac{1}{2}}} + \frac{\tau_2}{\tau} \frac{\partial}{\partial \tilde{U}_k} \frac{\tau_2}{\tau^{\frac{1}{2}}} = \frac{\tau_1}{\tau} \frac{k_1}{k} T_k + \frac{\tau_2}{\tau} \frac{k_2}{k} T_k.$$

Therefore, if τ_i is nonlinear

$$\frac{\partial}{\partial \tilde{U}_k} \tau_i = \tau^{\frac{1}{2}} \frac{k_i}{k} T_k + \frac{\tau_i}{\tau^{\frac{1}{2}}} \frac{\partial}{\partial \tilde{U}_k} \tau^{\frac{1}{2}}.$$

This implies that

$$\left\langle \frac{\partial}{\partial \tilde{U}_k} \tau_1 \right\rangle = \left\{ \left\langle \tau^{\frac{1}{2}} + \frac{\tau_1^2}{\tau^{\frac{3}{2}}} \right\rangle \frac{k_1}{k} + \left\langle \frac{\tau_1 \tau_2}{\tau^{\frac{3}{2}}} \right\rangle \frac{k_2}{k} \right\} T_k = \left\{ \left\langle t + \frac{t_1^2}{k} \right\rangle \frac{k_1}{k} + \left\langle \frac{t_1 t_2}{t} \right\rangle \frac{k_2}{k} \right\} T_k,$$

and analogously for τ_2.

A.3. *Average quantities*

All average quantities are computed relative to the coordinate system, which has $\sigma_{12} = 0$ and $\sigma_{22} \leqslant \sigma_{11}$. By definition

$$\langle t \rangle = \frac{1}{2\pi(\sigma_{11}\sigma_{22})^{\frac{1}{2}}} \int\int_{-\infty}^{+\infty} (t_1^2 + t_2^2)^{\frac{1}{2}} \exp\left[-\frac{1}{2}\left(\frac{t_1^2}{\sigma_{11}} + \frac{t_2^2}{\sigma_{22}} \right) \right] \mathrm{d}t_1 \, \mathrm{d}t_2.$$

Write

$$t_1 = \sigma_{11}^{\frac{1}{2}} s \cos\alpha, \quad t_2 = \sigma_{22}^{\frac{1}{2}} s \sin\alpha$$

and transform to the variables s, α:

$$\langle t \rangle = \frac{1}{2\pi} \int_0^{2\pi} \int_0^{\infty} (\sigma_{11}\cos^2\alpha + \sigma_{22}\sin^2\alpha)^{\frac{1}{2}} s^2 \exp(-\tfrac{1}{2}s^2) \, \mathrm{d}s \, \mathrm{d}\alpha$$

$$= \frac{\sigma_{11}^{\frac{1}{2}}}{\pi} \int_0^1 (1-Ar)^{\frac{1}{2}} (1-r)^{-\frac{1}{2}} r^{-\frac{1}{2}} \mathrm{d}r \int_0^{\infty} s^2 \exp(-\tfrac{1}{2}s^2) \, \mathrm{d}s.$$

with $A = 1 - \sigma_{22}/\sigma_{11}$ and $r = \sin^2\alpha$.

Evaluating these integrals (see Abramowitz & Stegun 1965, ch. 7 and 15) it is found that

$$\langle t \rangle = \sigma_{11}^{\frac{1}{2}} \tfrac{1}{2} (2\pi)^{\frac{1}{2}} F(-\tfrac{1}{2}, \tfrac{1}{2}, 1, A),$$

with F a hypergeometric function. In an analogous way:

$$\left\langle \frac{t_1^2}{t} \right\rangle = \sigma_{11}^{\frac{1}{2}} \tfrac{1}{4}(2\pi)^{\frac{1}{2}} F(\tfrac{1}{2}, \tfrac{1}{2}, 2, A),$$

$$\left\langle \frac{t_2^2}{t} \right\rangle = \langle t \rangle - \left\langle \frac{t_1^2}{t} \right\rangle,$$

$$\langle t^{\frac{1}{2}} \rangle = \sigma_{11}^{\frac{1}{4}} 2^{\frac{1}{4}} \Gamma(\tfrac{5}{4}) F(-\tfrac{1}{4}, \tfrac{1}{2}, 1, A),$$

$$\sigma_{12} = 0 \text{ implies that } \left\langle \frac{t_1 t_2}{t} \right\rangle = 0.$$

From Gauss' relations for contiguous hypergeometric functions it follows that

$$v_{11} = \left\langle t + \frac{t_1^2}{t} \right\rangle = \sigma_{11}^{\frac{1}{2}} \tfrac{3}{4}(2\pi)^{\frac{1}{2}} F(-\tfrac{1}{2}, \tfrac{1}{2}, 2, A),$$

$$v_{22} = \left\langle 2t - \frac{t_1^2}{t} \right\rangle = \sigma_{11}^{\frac{1}{2}} \tfrac{3}{4}(2\pi)^{\frac{1}{2}} F(-\tfrac{1}{2}, \tfrac{3}{2}, 2, A).$$

The nonlinear velocity v_t is now given by

$$\begin{aligned} v_t &= v_{11} \frac{k_1'^2}{k^2} + v_{22} \frac{k_2'^2}{k^2} \\ &= v_{11}(\cos\theta \cos\phi + \sin\theta \sin\phi)^2 + v_{22}(\cos\theta \sin\phi - \sin\theta \cos\phi)^2 \\ &= v_{11} \cos^2(\theta - \phi) + v_{22} \sin^2(\theta - \phi), \end{aligned}$$

where k_1' and k_2' denote $k_1 (= k\cos\theta)$ and $k_2 (= k\sin\theta)$ relative to the rotated coordinate system, $\tilde{\theta} = \theta - \phi$ is the angle between a wave component and the main axis of the bottom stress spectrum.

The linear velocity v_t follows from

$$v_t = \langle t^{\frac{1}{2}} \rangle^2 = \sigma_{11}^{\frac{1}{2}} \sqrt{2}\, \Gamma(\tfrac{5}{4})^2 F(-\tfrac{1}{4}, \tfrac{1}{2}, 1, A)^2.$$

All hypergeometric functions used have a maximum of 1 at $A = 0$.

REFERENCES

Abramowitz, M. & Stegun, I. A. 1965 *Handbook of Mathematical Functions*. Dover.

Bakker, W. T. & Doorn, Th. van 1979 Near bottom velocities in waves with a current. In *Proc. 16th Intl Conf. on Coastal Engng 1978*, pp. 1394–1413. ASCE.

Beran, J. M. 1968 *Statistical Continuum Theories*. Interscience.

Bouws, E. & Komen, G. J. 1983 On the balance between growth and dissipation in an extreme depth-limited wind–sea in the southern North Sea. *J. Phys. Oceanogr.* **13**, 1653–1658.

Christoffersen, J. B. & Jonsson, I. G. 1985 Bed friction in a combined current and wave motion. *Ocean Engng* **12**, 387–423.

Collins, J. I. 1972 Prediction of shallow water spectra. *J. Geophys. Res.* **93** (C1), 491–508.

Davies, A. G., Soulsby, R. L. & King, H. L. 1988 A numerical model of the combined wave and current bottom boundary layer. *J. Geophys. Res.* **93** (C1), 491–508.

Dyer, K. R. & Soulsby, R. L. 1988 Sand transport on the continental shelf. *Ann. Rev. Fluid Mech.* **20**, 295–324.

Grant, W. D. & Madsen, O. S. 1979 Combined wave and current interaction with a rough bottom. *J. Geophys. Res.* **84** (C4), 1797–1808.

GRANT, W. D. & MADSEN, O. S. 1982 Movable bed roughness in unsteady oscillatory flow. *J. Geophys. Res.* **87** (C1), 469–481.

HASSELMANN, K. & COLLINS, J. I. 1968 Spectral dissipation of finite depth gravity waves due to turbulent bottom friction. *J. Mar. Res.* **26**, 1–12.

HINO, M., KASHIWAYANAGI, M., NAKAYAMA, A. & HARA, T. 1983 Experiments on the turbulence statistics and the structure of a reciprocating oscillatory flow. *J. Fluid Mech.* **131**, 363–400.

HORIKAWA, K. & WATANABE, A. 1968 Laboratory study on oscillatory boundary layer flow. *Coastal Engng Japan* **11**, 13–28.

HUNTLEY, D. A. & HAZEN, D. G. 1988 Seabed stresses in combined wave and steady flow conditions on the Nova Scotia continental shelf: field measurements and predictions. *J. Phys. Oceanogr.* **19**, 347–362.

JONSSON, I. G. 1980 A new approach to oscillatory rough turbulent boundary layers. *Ocean Engng* **7**, 109–152.

JONSWAP: HASSELMANN, K., BARNETT, T. P., BOUWS, E., CARLSON, H., CARTWRIGHT, D. E., ENKE, K., EWING, J. A., GIENAPP, H., HASSELMANN, D. E., KRUSEMAN, P., MEERBURG, A., MÜLLER, P., OLBERS, D. J., RICHTER, K., SELL, W. & WALDEN, H. 1973 Measurements of wind–wave growth and swell decay during the Joint North Sea Wave Project (JONSWAP). *Dtsch. Hydrogr. Z.* **A8** (12), 95.

KAJIURA, K. 1968 A model of the bottom boundary layer in water waves. *Bull. Earthquake Res. Inst.* **46**, 75–123.

LAVELLE, J. W. & MOFJELD, H. O. 1983 Effects of time-varying viscosity on oscillatory turbulent channel flow. *J. Geophys. Res.* **88** (C12), 7607–7616.

LONGUET-HIGGINS, M. S. 1963 The effect of nonlinearities on statistical distributions in the theory of sea waves. *J. Fluid Mech.* **17**, 459–480.

MADSEN, O. S., POON, Y.-K. & GRABER, H. C. 1989 Spectral wave attenuation by bottom friction: theory. In *Proc. 21st Conf. on Coastal Engng 1988*, pp. 492–504. ASCE.

NAYFEH, A. H. 1973 *Perturbation Methods*. Wiley Interscience.

RICE, S. O. 1944 The mathematical analysis of random noise. *Bell Syst. Tech. J.* **23**, 282–332.

RICE, S. O. 1945 The mathematical analysis of random noise. *Bell Syst. Tech. J.* **24**, 46–156.

SCHLICHTING, H. 1955 *Boundary Layer Theory*. McGraw Hill.

SHEMDIH, O., HASSELMANN, K., HSIAO, S. V. & HERTERICH, K. 1978 Non-linear and linear bottom interaction effects in shallow water. In *Turbulent Fluxes through the Sea Surface, Wave Dynamics and Prediction. NATO Conf. Ser. V*, Vol. 1, pp. 647–665. Plenum.

SLEATH, J. F. A. 1987 Turbulent oscillatory flow over rough beds. *J. Fluid Mech.* **182**, 369–409.

TENNEKES, H. & LUMELY, J. L. 1972 *A First Course in turbulence*. The MIT Press.

TROWBRIDGE, J. & MADSEN, O. S. 1984 Turbulent wave boundary layers, 1. Model formulation and first order solution. *J. Geophys. Res.* **89** (C5), 7989–7999.

VISSER, M. 1988 Energiedissipatie van zeegolven in de turbulente bodemgrenslaag. Sc.D. thesis. KNMI *Tech. Rep.* TR-104. De Bilt, The Netherlands (in Dutch).

WAMDI GROUP 1988 The WAM model – A third generation ocean wave prediction model. *J. Phys. Oceanogr.* **18**, 1775–1810.

WEBER, S. L. 1988 The energy balance of finite depth gravity waves. *J. Geophys. Res.* **93** (C4), 3601–3607.

WEBER, S. L. 1989 Surface gravity waves and turbulent bottom friction. Ph.D. thesis, University of Utrecht.

WEBER, S. L. 1991 Bottom friction for wind–sea and swell in extreme depth-limited situations. *J. Phys. Oceanogr.* **21**, 149–172.

WILSON, K. C. 1989 Friction of wave-induced sheet flow. *Coastal Engng* **12**, 371–379.